Neurobiology of Aging 81 (2019) 222–233

Contents lists available at ScienceDirect

Neurobiology of Aging

journal homepage: www.elsevier.com/locate/neuaging

Reduced sensory-evoked structural plasticity in the aging barrel cortex

Rebecca L. Voglewede [a,b,c], Kaeli M. Vandemark [a,b], Andrew M. Davidson [c,d], Annie R. DeWitt [a,b], Marissa D. Heffler [a,b,e], Emma H. Trimmer [c], Ricardo Mostany [a,b,c,*]

[a] Neuroscience Program, Tulane University School of Science and Engineering, New Orleans, LA, USA
[b] Tulane Brain Institute, Tulane University, New Orleans, LA, USA
[c] Department of Pharmacology, Tulane University School of Medicine, New Orleans, LA, USA
[d] Department of Cell and Molecular Biology, Tulane University School of Science and Engineering, New Orleans, LA, USA
[e] Department of Biomedical Engineering, Tulane University School of Science and Engineering, Lindy Boggs Center Suite 500, New Orleans, LA, USA

ARTICLE INFO

Article history:
Received 21 December 2018
Received in revised form 15 June 2019
Accepted 15 June 2019
Available online 26 June 2019

Keywords:
Dendritic spine
Primary somatosensory cortex
Two-photon imaging
Structural plasticity
Aging
Clustering

ABSTRACT

Impairments in synaptic connectivity have been linked to cognitive deficits in age-related neurodegenerative disorders and healthy aging. However, the anatomical and structural bases of these impairments have not been identified yet. A hallmark of neural plasticity in young adults is short-term synaptic rearrangement, yet aged animals already display higher synaptic turnover rates at the baseline. Using two-photon excitation (2PE) microscopy, we explored if this elevated turnover alters the aged brain's response to plasticity. Following a sensory-evoked plasticity protocol involving whisker stimulation, aged mice display reduced spine dynamics (gain, loss, and turnover), decreased spine clustering, and lower spine stability when compared to young adult mice. These results suggest a deficiency of the cortical neurons of aged mice to structurally incorporate new sensory experiences, in the form of clustered, long-lasting synapses, into already existing cortical circuits. This research provides the first evidence linking experience-dependent plasticity with in vivo spine dynamics in the aged brain and supports a model of both reduced synaptic plasticity and reduced synaptic tenacity in the aged somatosensory system.

1. Introduction

Increasing age is linked with several sensory deficits including elevated thresholds for stimulus detection and discrimination (Patel and Larson, 2009; Thornbury and Mistretta, 1981) and decreased somatosensory gating (Spooner et al., 2018) even in the absence of overt neuropathological changes. An overarching hypothesis within the aging field is that neural plasticity is compromised (for reviews, see Foster, 1999; Burke and Barnes, 2006; Greenwood, 2007), resulting in diminished aptitude for learning and flexibility in the aged brain and leading to age-related cognitive impairment. However, the anatomical substrate of this diminished plasticity is unclear, and how this age-related deficit shapes the response to sensory experience remains unknown.

One likely target modified during aging is the postsynaptic dendritic spine, a small protrusion from the dendritic shaft of neurons. These spines receive the majority of excitatory input in the brain; therefore, their arrangements and structural dynamics are canonically used as proxy for excitatory synapse function (Harris and Stevens, 1989; Wilbrecht et al., 2010). Changes involving spine number, stability, and structure can indicate pathological changes in the cortex (Bloss et al., 2013; Spires-Jones et al., 2007; Sweet et al., 2009). Equally importantly, the same changes to spines can also serve as an anatomical index of experience and learning, as has been shown in the primary somatosensory cortex where pyramidal neurons commonly receive both local (Hooks et al., 2011) and long-range input from several areas including the ventral posterior medial and posterior medial nuclei of the thalamus (Constantinople and Bruno, 2013; Gambino et al., 2014; Mease et al., 2016b,a; Williams and Holtmaat, 2019; Zhang and Bruno, 2019), the secondary somatosensory cortex (Cauller et al., 1998), and the primary motor cortex (Lee et al., 2013; Petreanu et al., 2012, 2009; Veinante and Deschênes, 2003). Furthermore, spatial distribution of spines along the dendritic shaft is not random: spine clustering is emerging as a higher-order organizational arrangement of synaptic contacts given that it may allow for nonlinear summation of synaptic inputs (Larkum and Nevian, 2008) and facilitate cross-talk between

* Corresponding author at: Department of Pharmacology, Tulane University School of Medicine, 1430 Tulane Avenue, Mail Code 8683, New Orleans, LA 70112, USA. Tel.: +1 504 988 6623; fax: +1 504 988 5283.
E-mail address: rmostany@tulane.edu (R. Mostany).

0197-4580/$ – see front matter © 2019 Elsevier Inc. All rights reserved.
https://doi.org/10.1016/j.neurobiolaging.2019.06.006

synapses after induction of LTP (Harvey and Svoboda, 2007). An impaired plasticity hypothesis of aging predicts that the structural plasticity in S1 of young adult mice that occurs in response to sensory stimulation should be reduced or absent in aged mice exposed to the identical stimulation. Very few studies have explored in vivo spine dynamics in the context of aging, and no studies to date have explored the impact of aging on in vivo experience-dependent structural plasticity at the level of the dendritic spines.

In this study, we use in vivo 2PE laser scanning microscopy to track the dynamics of spines over a period of as many as 46 days before, during, and after whisker stimulation in young and aged mice to identify the extent to which aging impacts the ability of sensory inputs to modify spine dynamics and clustering. We hypothesize that elevated steady-state spine turnover in aged animals (Mostany et al., 2013) is linked with decreased structural plasticity after sensory stimulation. In young adult mice, whisker stimulation evokes a rapid and short-term but robust increase in spine dynamics that then falls back to steady-state levels. In aged mice, whisker stimulation results in a long-lived decrease in spine dynamics that is smaller in magnitude and detectable only after multiple sessions of sensory stimulation. Although the decrease in spine dynamics could be interpreted as a form of synaptic stabilization for aged mice, they show no improvements in the stability of individual spines and a decrease in spine clustering, an indicator of synaptic strengthening. Thus, although sensory stimulation produces a decrease in synaptic fluctuation for aged mice, this effect does not improve spine persistence or rearrangement associated with long-lasting memories. Together, these data support a model of steady-state synaptic instability in aged mice leading to suboptimal incorporation of sensory experience.

2. Methods

2.1. Animals

Thy1-eGFP-M mice (The Jackson Laboratory, 007788, Tg (Thy1-EGFP)MJrs/J; RRID:IMSR_JAX:007788; Feng et al., 2000), aged 3–5 months (young adult) and 18–21 months (aged), were used for experiments. Only male mice were used in this study, as it was recently reported (Alexander et al., 2018) that the estrous cycle may have effects on sensory-evoked plasticity. Food and water were provided *ad libitum* and mice were group-housed under a 12-hour light/dark cycle. All procedures were approved by the Tulane University Institutional Care and Use Committee and were performed in accordance with the NIH Office of Laboratory Animal Welfare's Public Health Service Policy on Humane Care and Use of Laboratory Animals and Guide for the Care and Use of Laboratory Animals.

2.2. Cranial window surgery

Cranial window surgery was performed as previously described (Holtmaat et al., 2009; Mostany et al., 2013; Mostany and Portera-Cailliau, 2008). Mice were anesthetized with isoflurane (5.0% for induction, 1.5%–1.7% for maintenance) and given subcutaneous injections of carprofen (5.0 mg/kg; Zoetis Inc) and dexamethasone (0.2 mg/kg; MWI) to prevent brain swelling and inflammation. Mice were placed in a stereotaxic frame, and a 4 mm craniotomy was performed with a pneumatic dental drill over the barrel field of the primary somatosensory cortex (S1BF), centered at 3 mm lateral to the midline and 1.95 mm caudal to bregma. A 5 mm glass coverslip (#1; Electron Microscopy Sciences) was placed over the intact dura and secured with cyanoacrylate glue and dental acrylic (Lang Dental Mfg. Co, Inc) to the skull. A custom-made titanium bar (9.5 × 3.2 × 1.1 mm) was cemented within the dental acrylic for fixing the mouse to the microscope's stage. A 2- to 3-week recovery time was allowed before imaging.

2.3. Intrinsic optical signal imaging

Mice were anesthetized with isoflurane (5.0% for induction, 1.0% for imaging) and secured to a custom-built intrinsic optical signal (IOS) microscope using the titanium bar. Imaging was done as described previously (Alexander et al., 2018; Johnston et al., 2013) through the cranial window preparation. An image of the vasculature was taken for reference under a green (535 nm) LED array, and the focus was placed 250–350 μm below the dura for the imaging. IOSs from S1BF were taken under 2 arrays of red (630 nm) LEDs using a fast camera (Pantera 1M60; Dalsa), frame grabber (64 Xcelera-CL PX4; Dalsa), and custom-written MATLAB (MathWorks; RRID: SCR_001622) routines while the whiskers were bundled and attached with dental wax to a glass capillary tube controlled by a piezo bender actuator (Physik Instrumente). Imaging sessions consisted of 30 trials of whisker stimulation for 1.5 seconds in the rostrocaudal direction at 10 Hz with 20-second breaks. Frames 0.9 seconds before onset of stimulation (baseline) and 1.5 seconds after stimulation (response) were collected. The response signal from each stimulation was divided by the baseline signal and summed to obtain the signal map. An outline of the IOS map was placed over the image of the vasculature to identify the activated cortical area. At the start of the chronic 2PE imaging, cells were chosen from within this activity map.

2.4. Chronic in vivo 2PE imaging

Mice were anesthetized with isoflurane (5.0% for induction, 1.0%–1.5% for imaging) and secured to a custom-built 2PE microscope using the titanium bar. Dendritic spine imaging (Alexander et al., 2018; Mostany et al., 2010, 2013) was done using a Ti:sapphire laser (Chameleon Ultra II; Coherent) tuned to 910 nm, a 40× 0.8 NA water-immersion objective (Olympus), and ScanImage software (RRID: SCR_014307; Pologruto et al., 2003) written in MATLAB. A reticle within the ocular of the microscope was used to identify the point of origin within the vascular map using both a 4× and 40× objective, after which the locations of individual dendritic fragments for a cell of interest were recorded using a coordinate system and micromanipulator controller (Sutter Instrument). Layer 5 (L5) pyramidal neurons were verified by a cell body depth of 400–700 μm below the dura. A selection of 5–8 dendritic fragments of the apical tuft were imaged chronically. High-magnification image stacks (0.14 × 0.15 μm/pixel; 1.5 μm apart) were collected for the analysis of dendritic spines. Imaged fragments were located within layer 1 (L1) and found at depths of 15–115 μm below the pia (average depth = −48.0 ± 2.0 μm, young adult; −51.0 ± 3.0 μm, aged, branch order is estimated ≥4th). These fragments were imaged chronically over imaging intervals of either 4 days (9 sessions total; 3 sessions before stimulation: −d8, −d4, d0; 3 sessions after stimulation: +d4, +d8, +d12; 3 sessions occurring 1 month after stimulation: +d30, +d34, +d38) or 24 hours (11 sessions total: 3 sessions before stimulation: −d2, −d1, d0; 4 throughout stimulation, +d1, +d2, +d3, +d4; 4 sessions after stimulation, +d5, +d6, +d7, +d8).

2.5. Whisker stimulation

Mice were anesthetized with isoflurane (5.0% for induction, < 1.0% during stimulation) and secured to a platform using the titanium bar. Whiskers were bundled and attached to a piezo bender actuator, which oscillated rostrocaudally at 8 Hz (Carvell and Simons, 1990) continuously for 10 minutes. The stimulation (Alexander et al.,

2018) was modeled after a previous study demonstrating physiological long-term plasticity via epicranial recordings in S1 (Megevand et al., 2009) and a similar adaptation recently linked with long-term potentiation (Gambino et al., 2014; Williams and Holtmaat, 2019) of pyramidal neurons within layer 2/3 of S1 using a whole-cell configuration. Stimulation was performed within 24 ± 1 hour for 4 consecutive days, on d0 (immediately after the imaging session), +d1, +d2, and +d3 within both the 4-day and 24-hour interval experimental timelines. For the 4d-interval experiment, we added a third group of mice—faux stimulation group—that is, young adult mice in which 2 piezoelectric actuators were used: one nonoscillating actuator, attached to the whiskers for the same time periods and duration, and a second unattached piezoelectric actuator situated 2 inches lateral and oscillated at the appropriate 8 Hz frequency to control for effects of extraneous sensory effects (e.g., vibration, noise) associated with the piezoelectric actuator.

2.6. Analysis

2.6.1. Spine dynamics analysis

Dendritic spine density and dynamics were determined from stacks of 2-D 2PE images using routines within ScanImage software (kindly provided by the Svoboda laboratory, Janelia Research Campus) written in MATLAB. All visible spines projecting 1/3 or beyond the cross-section of the adjacent dendritic shaft were manually scored, including those on the z-axis clearly protruding beyond the noise of the dendritic shaft. A minimum of 3 different dendritic fragments (regions of interest) and 100 identifiable spines were required for each cell; all cells not meeting these criteria were excluded from analysis. For the 4-day imaging interval timeline ending on +d12, we analyzed dendritic spines from $n = 18$ cells (from $N = 10$ young adult mice), $n = 20$ cells (from $N = 9$ aged mice), and $n = 6$ cells (from $N = 6$ young adult mice with faux stimulation). In an additional subset of mice ($n = 10$ cells [from $N = 6$ young adult mice] and $n = 14$ cells [from $N = 6$ aged mice]), imaging was extended to include +d30, +d34, and +d38. For the 24-hour imaging timeline, we analyzed dendritic spines from $n = 12$ cells (from $N = 6$ young adult mice) and $n = 12$ cells (from $N = 6$ aged mice). Together, we tracked a total of 8032 distinct dendritic spines over 6–11 imaging sessions. For display purposes only, best projections of the dendritic segments were obtained, where the best focal plane is identified and overlaid in Adobe Photoshop CC (Adobe Systems Inc; RRID: SCR_014199), preserving all the elements in the segment, and a median filter (radius of 2) was applied. We defined turnover rate (TOR) of dendritic spines as the combined number of gained and lost spines per unit length (μm) since the previous imaging day, and we expressed it as per 100 μm of dendrite ([#gained spines + #lost spines]/100 μm). The survival function of dendritic spines was obtained by fitting the survival fraction at the different time points to a single exponential decay curve.

2.6.2. Spine clustering analysis

To investigate dendritic spine clustering, a custom-written MATLAB routine (inspired by Yadav et al., 2012) was used to identify likely spine clusters (groups of 3 or more spines) based on proximity between spines. After each dendritic fragment was analyzed for spine density and dynamics, as explained previously, the length of the fragment, the coordinates of each spine, and the persistence identity of each spine (stable, gained, eliminated) were used to build a 2-D model of the fragment. Based on this model and a preset cluster threshold (the maximum distance allowed between 2 adjacent spines belonging to the same cluster) in microns, an agglomerative ("bottom up") hierarchical cluster tree was constructed using Euclidean as the distance metric and shortest distance method for linkage of dendritic spines. Multiple cluster trees were constructed for each fragment—one for every threshold value between 0.2 and 5.0 μm—with 0.2 μm increments. A "c-score" (Yadav et al., 2012) was used to select the most appropriate cluster threshold for every fragment and was calculated for each using the following approach: for each cluster threshold, a Monte Carlo simulation was run 5000 times in which the number of spines and length of the fragment were equal to the actual observed dendrite but the position of the spines along the fragment was randomized. Then a frequency distribution of the fraction of spines belonging to clusters in that particular dendrite fragment was generated. The point along the frequency distribution at which the observed dendrite fell was identified as that cluster threshold's "c-score" for that fragment. The lowest cluster threshold at which the c-score reached or surpassed 0.90 (not including reaching the maximum 1.0 value, at which all spines belong to a cluster) was used for calculation of other spine clustering metrics, and this fragment was categorized as a highly clustered fragment. If no cluster threshold existed at which the c-score criteria are met, the fragment was categorized as a minimally clustered fragment and was not used in further calculations.

2.6.3. Statistical analysis

Prestimulation statistical differences of spine dynamics between age groups were calculated with unpaired *t*-tests. Poststimulation statistical differences of spine dynamics within age groups were calculated with repeated-measures one-way ANOVA followed by Bonferroni post hoc tests to correct for multiple comparisons. Statistical differences between the measures of dendritic spine persistence were calculated using student's *t*-test and repeated-measures two-way ANOVA followed by Bonferroni post hoc tests to correct for multiple comparisons. For statistical analysis of the spine clustering data, we used Wilcoxon matched-pairs signed-rank and Mann-Whitney *U* test to account for non-normality (assessed using Shapiro-Wilk test) of the data followed by Bonferroni post hoc tests to correct for multiple comparisons. The differences in dendritic spine survival fractions and rate constant *K* were computed using extra sum-of-squares *F*-test. All statistical analyses were performed with GraphPad Prism (GraphPad Software; RRID: SCR_002798). All bar graphs are presented as mean ± SEM unless otherwise stated. All box-and-whisker-plots show minimum to maximum values and median values marked with horizontal lines and "+" indicating the mean. Significance was set at $p < 0.05$. In the figures, $^{*}p < 0.05$, $^{**}p < 0.01$, and $^{***}p < 0.001$.

3. Results

3.1. Steady-state spine dynamics are higher in aged mice

Before the introduction of sensory manipulation, we imaged for 3 sessions (−d8, −d4, d0; Fig. 1A) to obtain measurements of dendritic spine dynamics at the steady state for both young adult and aged mice (Fig. 1C). We used a 4-day interval (see experimental timeline, Fig. 1A) and sampled before and immediately after sensory manipulation (Fig. 1B) to examine short-term effects on structural plasticity. A comparison between age groups revealed a difference in prestimulation spine TORs (defined as spine gain + elimination per 100 μm of dendritic shaft) in L5 S1BF. Aged mice displayed higher TOR (16.5 ± 0.7 spines) than young adults (13.5 ± 0.8; $t_{(36)} = 2.781$, $p = 0.0086$; Fig. 1D), in agreement with our previous study on steady-state dynamics of spines in broad S1 (Mostany et al., 2013). These age-dependent differences were visible individually within spine gain (# spines gained per 100 μm of dendritic shaft; young adult: 6.6 ± 0.4, aged: 7.9 ± 0.4; $t_{(36)} = 2.28$, $p = 0.0286$; Fig. 1F) and spine elimination (# spines

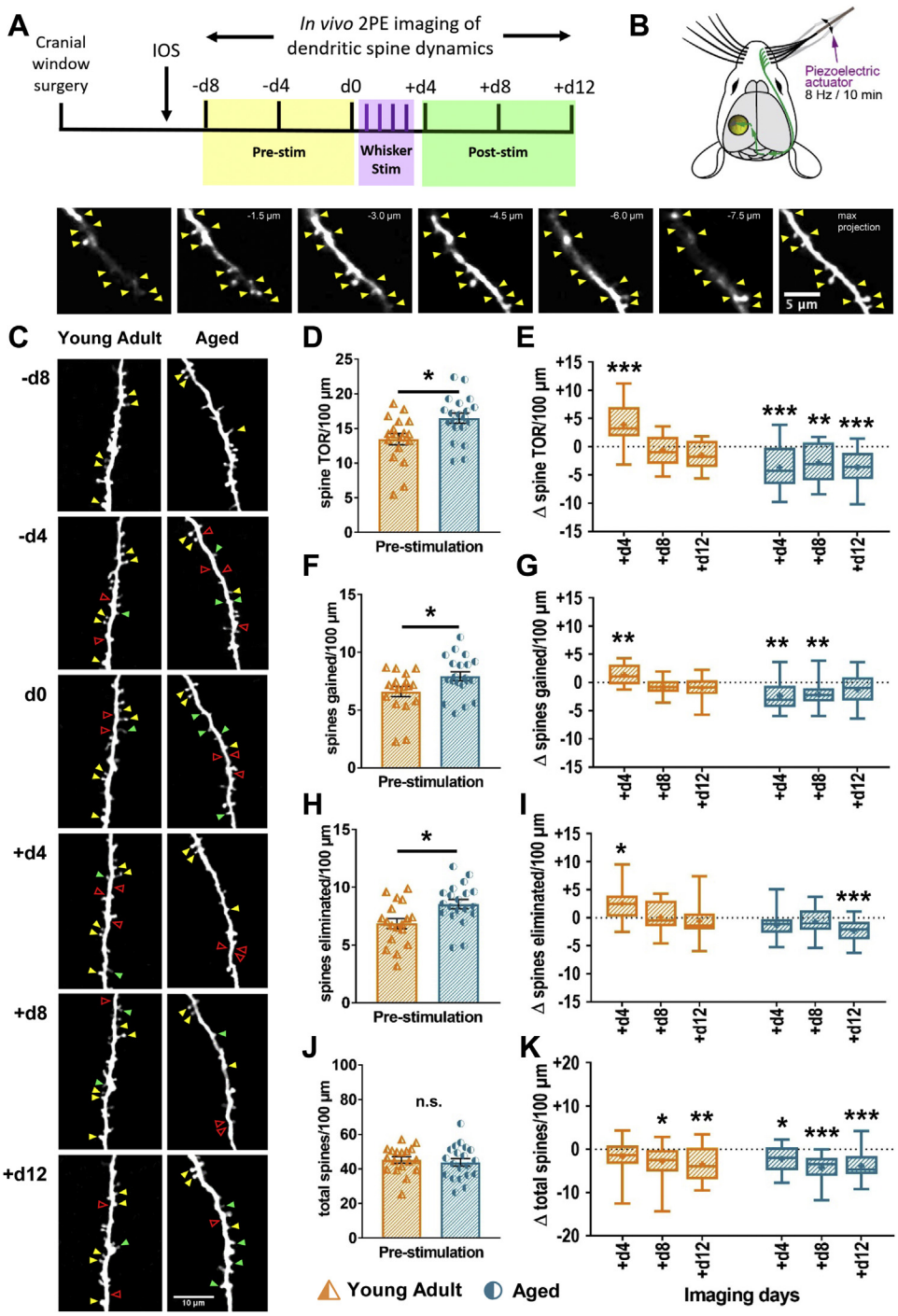

print & web 4C/FPO

Fig. 1. Young adult and aged mice experience divergent responses in spine dynamics after whisker stimulation. (A) Experimental timeline with imaging intervals of 4 days over 20 days (−d8 to +d12) and a representative high-resolution image Z-stack showing the same dendritic fragment at various depths. (B) Schematic of bundled whisker stimulation protocol which consisted of rostrocaudal deflections of the whiskers contralateral to the cranial window position at 8 Hz for 10 minutes for 4 consecutive days. (C) Representative high-resolution images of dendritic segments from the apical tuft of layer 5 pyramidal neurons acquired with in vivo two-photon microscopy. Examples of persistent (through all time points) spines (yellow arrowheads), gained spines (green arrowheads), and eliminated spines (red arrowheads) are shown. Young adult versus aged prestimulation dendritic spine TOR (D), gain (F), elimination (H), and density (J); unpaired *t*-tests. Post-stimulation (pre-stim. vs. +d4, +d8, +d12) dendritic spine TOR (E), gain (G), elimination (I), and density (K); repeated-measures one-way ANOVA with Bonferroni post hoc tests to correct for multiple comparisons. For all data sets: $n = 18$ cells/10 mice (young adult) and 20 cells/9 mice (aged); bar graphs are presented as mean ± SEM; box-and-whisker plots = min to max with median line, + indicates mean; $^{*}p < 0.05$, $^{**}p < 0.01$, $^{***}p < 0.001$. Abbreviations: IOS, intrinsic optical imaging; TOR, turnover rate.

eliminated per 100 µm of dendritic shaft; young adult: 6.9 ± 0.4, aged: 8.6 ± 0.4; $t_{(36)} = 2.871$, $p = 0.0068$; Fig. 1H). Spine density (# spines per 100 µm of dendritic shaft), however, was not different between ages at the steady state (young adult: 45.0 ± 2.0, aged: 44.0 ± 2.0; $t_{(36)} = 0.5063$, $p = 0.6157$; Fig. 1J). The roughly equal magnitude of spines gained and spines lost in each age group indicates that although aged mice display higher spine fluctuation, there is no net effect on absolute spine number.

3.2. Whisker stimulation elicits divergent effects on spine dynamics for young adult and aged mice

To induce structural plasticity in S1BF, we used a plasticity-inducing stimulation protocol (Alexander et al., 2018) that consisted of continuous, back-and-forth deflections of the whiskers at 8 Hz for 10 min/d for 4 consecutive days (d0, +d1, +d2, and +d3; Fig. 1A and B). IOS imaging was used to determine the area activated by whisker stimulation and then cells were subsequently selected from that area.

Spines of young adult mice showed increased TOR ($\Delta = +3.9 \pm 0.8$; $F_{(3, 51)} = 17.68$, $p < 0.0001$; Fig. 1E), gain ($\Delta = +1.3 \pm 0.4$; $F_{(3, 51)} = 8.416$, $p = 0.0332$; Fig. 1G), and elimination ($\Delta = +2.5 \pm 0.8$; $F_{(3, 51)} = 5.452$, $p = 0.0111$; Fig. 1I) compared to their steady-state levels at four days (+d4) after the initiation of the whisker stimulation. These spine dynamics then returned to steady-state levels by +d8 (TOR, $F_{(3, 51)} = 17.68$, $p > 0.9999$; Fig. 1E; gain, $F_{(3, 51)} = 8.416$, $p = 0.4156$; Fig. 1G; elimination, $F_{(3, 51)} = 5.452$, $p > 0.9999$; Fig. 1I). A group exposed to a faux whisker stimulation protocol (see Section 2) showed no deviation from prestimulation spine dynamics levels at any time point (p values, respectively, for +d4, +d8, and +d12 for TOR: > 0.9999, 0.1226, and 0.1784, $F_{(3, 15)} = 2.351$; for gained spines: > 0.9999, >0.9999, >0.9999, $F_{(3, 15)} = 0.1434$; and for eliminated spines: > 0.9999, 0.0537, 0.2045, $F_{(3, 15)} = 5.469$; not shown). These data indicate that the temporary increase in spine dynamics seen in young adult mice is specific to the whisker stimulation protocol.

Aged mice displayed an opposite reaction to the stimulation: their spine TOR was reduced (+d4 $\Delta = -3.6 \pm 0.9$, $F_{(3, 57)} = 7.386$,

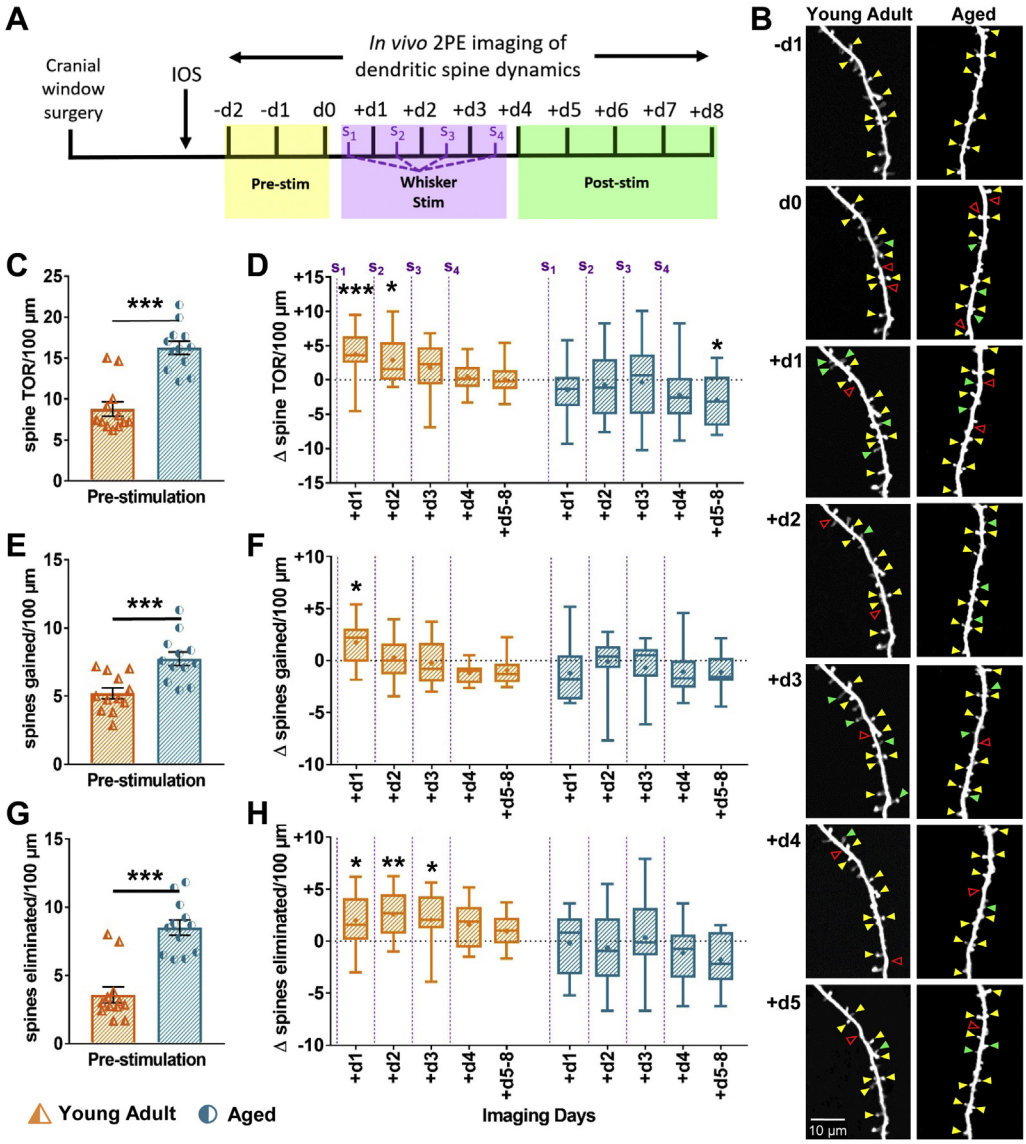

Fig. 2. The young adult response occurs rapidly for young adult mice but is more gradual for aged mice. (A) Experimental timeline with imaging intervals of 24 hours over 11 days (−d2 to +d8). (B) Representative high-resolution images of dendritic segments from the apical tuft of layer 5 pyramidal neurons acquired with in vivo two-photon microscopy. Examples of persistent (through all time points) spines (yellow arrowheads), gained spines (green arrowheads), and eliminated spines (red arrowheads) are shown. Young adult versus aged prestimulation dendritic spine TOR (C), gain (E), and elimination (G); unpaired *t*-tests. Post-stimulation (pre-stim. vs. +d1, +d2, +d3, +d4, +d5−8) dendritic spine TOR (D), gain (F), and elimination (H); repeated-measures one-way ANOVA with Bonferroni post hoc tests to correct for multiple comparisons. For all data sets: $n = 12$ cells/6 mice for each age group; bar graphs are presented as mean ± SEM; box-and-whisker plots = min to max with median line, + indicates mean, $^{*}p < 0.05$, $^{**}p < 0.01$, $^{***}p < 0.001$. Abbreviations: IOS, intrinsic optical imaging; TOR, turnover rate; $S_{1\text{-}4}$, whisker stimulation sessions (1–4).

$p = 0.0004$; Fig. 1E) and this reduction lasted through both +d8 ($\Delta = -2.8 \pm 0.8$, $F_{(3, 57)} = 7.386$, $p = 0.0088$; Fig. 1E) and +d12 ($\Delta = -3.6 \pm 0.7$, $F_{(3, 57)} = 7.386$, $p = 0.0005$; Fig. 1E). When broken down into spine gain versus elimination, the reduction in spine gain was already detectable at +d4 ($\Delta = -2.3 \pm 0.6$, $F_{(3, 57)} = 5.005$, $p = 0.0027$; Fig. 1G) and lasted through +d8 ($\Delta = -2.1 \pm 0.6$, $F_{(3, 57)} = 5.005$, $p = 0.0079$; Fig. 1G). A reduction in spine elimination appeared at +d12 ($\Delta = -2.3 \pm 0.5$, $F_{(3, 57)} = 5.347$, $p = 0.0009$; Fig. 1I).

Spine density decreased for both age groups after whisker stimulation. In young adult mice, the density decrease was visible by +d8 ($\Delta = -2.7 \pm 1.0$, $F_{(3, 51)} = 5.563$, $p = 0.0107$; Fig. 1K) and +d12 ($\Delta = -3.4 \pm 1.0$, $F_{(3, 51)} = 5.563$, $p = 0.0011$; Fig. 1K). The faux stimulation group does not show any deviation from prestimulation density at any time point (p values = 0.2870, 0.7302, 0.6347, $F_{(3, 15)} = 1.148$, for +d4, +d8, +d12, respectively; not shown) suggesting that the whisker stimulation protocol affects spine density via a larger increase in spine elimination than spine gain at +d4. The density decrease in aged mice is visible by +d4 ($\Delta = -2.2 \pm 0.7$, $F_{(3, 57)} = 13.22$, $p = 0.0148$; Fig. 1K) and persists through both +d8 ($\Delta = -4.3 \pm 0.7$, $F_{(3, 57)} = 13.22$, $p < 0.0001$; Fig. 1K) and +d12 ($\Delta = -3.9 \pm 0.8$, $F_{(3, 57)} = 13.22$, $p < 0.0001$; Fig. 1K). This rapid effect is mostly likely due to a decrease in new spines added, as the decrease in density (-2.2 ± 0.7; Fig. 1K) at +d4 is approximately equal to the concurrent decrease in spine gain (-2.3 ± 0.6; Fig. 1G).

3.3. Divergence in spine dynamics occurs after a single stimulation session for young adult mice but more gradually for aged mice

To observe changes in the dynamics of dendritic spines after individual stimulation sessions, we performed imaging at 24-hour intervals in an additional set of mice before, throughout, and after stimulation for a total of 11 consecutive days (Fig. 2A and B). Steady-state spine dynamics within 24-hour intervals (Fig. 2C,E and G) mirrored the age-dependent differences present at 4-day intervals (Fig. 1D,F and H). Aged mice displayed higher TOR (young adult: 8.8 ± 0.9, aged: 16.3 ± 0.8, $t_{(22)} = 6.249$, $p < 0.0001$; Fig. 2C), gain (young adult: 5.2 ± 0.4, aged: 7.7 ± 0.5, $t_{(22)} = 3.934$, $p = 0.0007$; Fig. 2D), and elimination (young adult: 3.6 ± 0.6, aged: 8.5 ± 0.6, $t_{(22)} = 6.038$, $p < 0.0001$; Fig. 2E) before any stimulation was introduced.

Young adult mice exhibited increased TOR ($\Delta = +4.0 \pm 1.0$, $F_{(5, 55)} = 5.957$, $p = 0.0007$; Fig 2D), gain ($\Delta = +1.7 \pm 0.6$, $F_{(5, 55)} = 6.803$, $p = 0.0151$; Fig. 2F), and elimination ($\Delta = +2.0 \pm 0.8$, $F_{(5, 55)} = 3.485$, $p = 0.0308$; Fig. 2H) at +d1, only 24 hours after the initiation of the whisker stimulation and after a single stimulation session (s_1). Spine TOR remained elevated through +d2 ($\Delta = +3.0 \pm 1.0$, $F_{(5, 55)} = 5.957$, $p = 0.0131$; Fig. 2D). This is likely due to increased spine elimination which remained elevated for +d2 ($\Delta = +2.6 \pm 0.6$, $F_{(5, 55)} = 3.485$, $p = 0.0024$; Fig. 2H) and +d3 ($\Delta = +2.1 \pm 0.8$, $F_{(5, 55)} = 3.485$, $p = 0.0248$; Fig. 2H), whereas spine gain returned to steady-state levels by +d2 ($\Delta = +0.3 \pm 0.6$, $F_{(5, 55)} = 6.803$, $p > 0.9999$; Fig. 2F).

In aged mice, spine TOR decreased at +d5–8 (Δ: -3.0 ± 1.0, $F_{(5, 55)} = 2.278$, $p = 0.0393$; Fig. 2D), but this is not reflected individually within spine gain (Δ: -1.1 ± 0.5, $F_{(5, 55)} = 1.156$, $p = 0.5968$; Fig. 2F) nor elimination (Δ: -1.8 ± 0.7, $F_{(5, 55)} = 1.662$, $p = 0.2178$; Fig. 2H). These data collectively suggest that the effect of whisker stimulation in young adult mice seen at 4-day intervals can be observed acutely and after only a single stimulation, while the reduction in spine dynamics in aged animals is subtle and thus only observed over a longer timeframe when combinatorial (spine gain + elimination), cumulative (multiple stimulation sessions), or both effects can be detected.

3.4. The effect of whisker stimulation on spine dynamics in aged mice persists for up to 1 month

We carried out an extended imaging timeline in a subset of mice from both age groups to determine if the effects that occurred shortly after whisker stimulation (+d4 through +d12) persisted for 30 days after the whisker stimulation (+d30 through +d38; Fig 3A and B). Young adult mice showed no differences from their steady-state levels of spine TOR, gain, and elimination after 30 days (Fig. 3C,D and E). These data suggest that the increase in spine fluctuation on +d4 is indeed temporary and the return to steady-state levels by +d8 is maintained.

Aged mice, however, showed a persistent deceleration from steady levels of spine TOR 30 days after the whisker stimulation (Δ: -2.6 ± 1.0, $t_{(13)} = 2.658$, $p = 0.0197$; Fig. 3C), likely due to an enduring reduction in spine gain (Δ: -1.3 ± 0.5, $t_{(13)} = 2.556$, $p = 0.0239$; Fig. 3D) rather than spine elimination (Δ: -1.3 ± 0.6, $t_{(13)} = 2.153$, $p = 0.0506$; Fig. 3E). These data suggest that the reduction in spine dynamics in aged mice after whisker stimulation is longer-lasting. It is possible that the delayed reduction in spine elimination seen at +d12 would present again but was not captured within our experimental timeframe. In combination with the 24-hour data, this extended timeline suggests that although the effect in aged mice may be more gradual (visible only by +d5–8), it is also longer-lasting.

3.5. Aged mice exhibit decreased spine persistence after whisker stimulation

Because the decrease in spine fluctuations displayed by aged mice could be an indicator of synapse stabilization, we examined the persistence of newly formed spines both before and after the introduction of whisker stimulation. We defined new persistent spines as newly identified spines that persist for at least an additional imaging session (4 days apart) per 100 μm. Although the densities of these persistent spines were similar between age groups before whisker stimulation (−d4; young adult: 4.6 ± 0.5; aged: 4.9 ± 0.4; $F_{(1, 36)} = 8.913$, $p > 0.9999$; Fig. 4A), aged mice displayed a significantly lower persistent spine density than young adult mice after whisker stimulation (+d4: young adult: 5.0 ± 0.4, aged: 3.3 ± 0.4, $F_{(1, 36)} = 8.913$, $p = 0.0260$; Fig. 4A). This difference was due to a decrease in persistence of spines in aged mice from their prestimulation levels ($F_{(1, 36)} = 8.913$, $p = 0.0044$, RM two-way ANOVA with Bonferroni post hoc; Fig. 4A). As spines persisting for 8+ days have been linked with the successful formation of synapses (Holtmaat et al., 2006), we extended this analysis to new spines formed after stimulation (first observed on +d4) lasting 8+ days (through +d12), for which the persistence of spines in young adult mice was still higher than in aged mice (young adult: 3.7 ± 0.3, aged: 2.6 ± 0.4, $t_{(36)} = 2.305$, $p = 0.0271$; Fig. 4B). Finally, we examined the rate of elimination of all spines present on the very first imaging session (−d8), regardless of their absolute lifetimes, that remained throughout the entire duration of the experiment. The percentage of spines that survived was similar for each age group (young adult: 52.0% ± 2.0%, aged: 49.0 ± 2.0%; $t_{(42)} = 1.202$, $p = 0.2360$; Fig. 4C). However, the spines of young adult mice exhibited a slower rate constant of decay (K = 0.0361 ± 0.0010) than those of aged mice (K = 0.041 ± 0.001, $F_{(1, 226)} = 10.05$, $p = 0.0017$; Fig 4C), which translates into a longer half-life (19.2 days for young adult vs. 16.87 days for aged). Interestingly, when these parameters were compared between young adult mice exposed to whisker stimulation and mice that underwent faux stimulation, the real whisker stimulation was linked with a longer half-life and slower constant rate of decay than the faux stimulation (faux stim: 16.58 days half-life; K = 0.042 ± 0.002; $F_{(1, 142)} = 6.324$, $p = 0.013$;

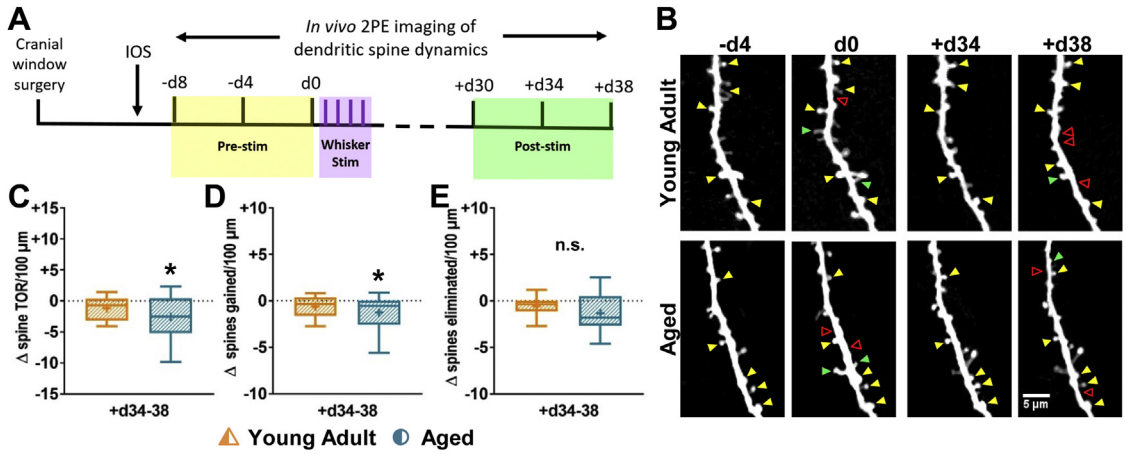

Fig. 3. Reduction in spine dynamics in aged mice lasts for more than 1 month after whisker stimulation. (A) Experimental timeline with imaging intervals of 4 days over a span of 46 days (−d8 to d0 and +d30 to +d38). (B) Representative high-resolution images of dendritic segments from the apical tuft of layer 5 pyramidal neurons acquired with in vivo two-photon microscopy. Examples of persistent (through all time points) spines (yellow arrowheads), gained spines (green arrowheads), and eliminated spines (red arrowheads) are shown. Post-stimulation (pre-stim. vs. +d34–38) dendritic spine TOR (C), gain (D), and elimination (E); paired *t*-tests. For all data sets: $n = 10$ cells/6 mice (young adult) and 14 cells/6 mice (aged); box-and-whisker plots = min to max with median line, + indicates mean; $^{*}p < 0.05$. Abbreviations: IOS, intrinsic optical imaging; TOR, turnover rate.

not shown). Thus, the differences in spine persistence observed between age groups may be due to the successful incorporation of a structural memory trace associated with the whisker stimulation by the young adult but not by the aged mice.

3.6. Young adult and aged mice display similar clustering characteristics in steady-state conditions

The data thus far examine spine activity in terms of population-level formation and elimination of spines. However, the spatial arrangement of these spines along the dendrite has large implications for how incoming information is integrated owing to a combination of passive and active dendritic properties. Higher prelearning spine turnover was recently linked with enhanced learning and spine stabilization via an increase in spine clustering in the young adult prefrontal cortex (Frank et al., 2018) and aged rats treated with the glutamate modulator riluzole demonstrated increased memory performance and lower cognitive decline that correlated with increased spine clustering in the hippocampus (Pereira et al., 2014). Given the higher steady-state TOR in aged mice, we examined spine clustering (see Section 2) both before (−d4) and after (+d4) whisker stimulation to see if experience-dependent plasticity would result in increased clustering of spines for aged mice in S1BF.

Before stimulation, dendritic fragments from both group ages classified as highly clustered (see Section 2) reveal similar characteristics. Clusters found within dendritic segments from young adult and aged mice contain approximately equal numbers of spines per cluster (young adult: 6.6 ± 0.6, aged: 6.0 ± 0.3, $U = 576.5$, $p > 0.9999$; Fig 5A). In addition, both age groups exhibit a similar density of clusters (# clusters/100 µm; young adult: 6.2 ± 0.4, aged: 6.6 ± 0.3, $U = 619.0$, $p > 0.9999$; Fig 5B), while the average individual cluster spans a similar length of dendrite (young adult: 10.0 ± 1.0 µm, aged mice: 9.0 ± 0.6 µm, $U = 570.0$, $p > 0.9999$; Fig 5C).

3.7. Cluster density after whisker stimulation decreases for aged mice, and spine rearrangement occurs more often outside of clusters

After whisker stimulation, the number of spines per cluster (young adult: 6.0 ± 0.5, $W = -89$, $p > 0.9999$; aged: 5.9 ± 0.3, $W = -161$, $p > 0.9999$; Fig 5A) and average cluster length (young adult: 9.0 ± 1.0, $W = -181$, $p = 0.0816$; aged: 8.4 ± 0.7, $W = -241$, $p = 0.7092$; Fig 5B) remain static for both age groups. The density of clusters along the dendrite, however, decreases for aged mice (5.6 ± 0.4, $W = -421$, $p = 0.0308$, Fig. 5C).

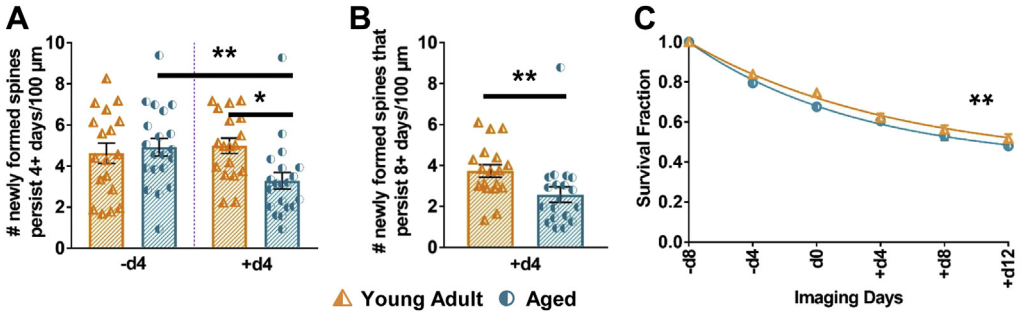

Fig. 4. Reduced spine dynamics in aged mice is not coupled with increased spine persistence. (A) Density of new spines on either −d4 (formed before stimulation) or +d4 (formed after stimulation) persisting for 4+ days. Repeated-measures two-way ANOVA with Bonferroni post hoc tests to correct for multiple comparisons. (B) Density of new spines formed on +d4 persisting for 8+ days. Unpaired *t*-test. (C) Survival fraction of total spines present on −d8 for the duration of the experiment comparing rate of decay, *K*. Nonlinear regression with one-phase decay followed by extra sum-of-squares *F* test. For all data sets: $n = 18$ cells/10 mice (young adult) and 20 cells/9 mice (aged); bar graphs are presented as mean ± SEM; $^{*}p < 0.05$, $^{**}p < 0.01$.

print & web 4C/FPO

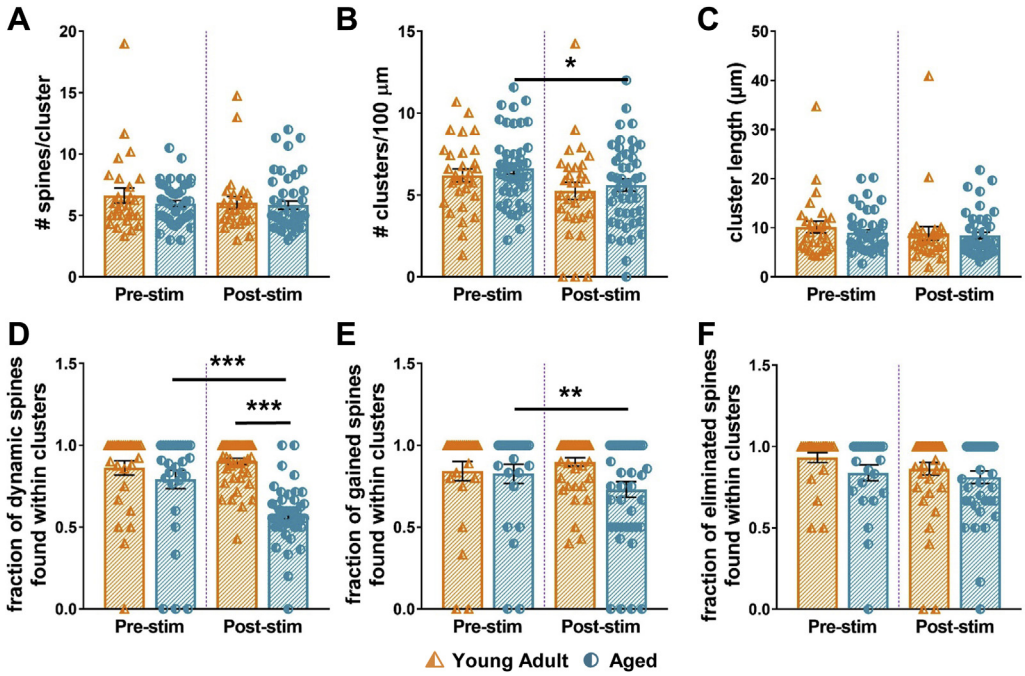

Fig. 5. Spine cluster density decreases and rearrangement within clusters decreases in aged mice after stimulation. Analysis of spine clustering before stimulation (−d4) versus after stimulation (+d4). (A) Spines per cluster. (B) Clusters/100 µm. (C) Cluster length. (D) Fraction of dynamic spines found within clusters. (E) Fraction of spines gained within clusters. (F) Fraction of spines eliminated from clusters. For all data sets: Wilcoxon matched-pairs signed-rank tests for within-group comparisons and Mann-Whitney *U* test for between-group comparisons, all with Bonferroni post hoc tests to correct for multiple comparisons; for data sets A and C: $n = 27$ fragments/12 cells/9 mice (young adult) and 45 fragments (18 cells/9 mice (aged); for B and D: $n = 30$ fragments/12 cells/9 mice (young adult) and 46 fragments (18 cells/9 mice (aged); For E: $n = 26$ fragments/11 cells/8 mice (young adult) and 43 fragments (18 cells/9 mice (aged); For F: $n = 25$ fragments/11 cells/8 mice (young adult) and 41 fragments (16 cells/8 mice (aged); bar graphs are presented as mean ± SEM; $^{*}p < 0.05$, $^{**}p < 0.01$, $^{***}p < 0.001$.

Given that this decreased clustering is coupled with a concurrent decrease in spine dynamics for aged mice (see +d4 data in Fig. 1), we examined whether the spine dynamics we observed are happening within clusters or outside of them by examining the population of dynamic spines (i.e., spines that appeared or disappeared). Before whisker stimulation, the fraction of dynamic spines that were gained into or eliminated from clusters was similar for both age groups (young adult: 0.86 ± 0.04, aged: 0.90 ± 0.02; $U = 669.5$, $p > 0.9999$; Fig. 5D). After whisker stimulation, the proportion of dynamic spines occurring within clusters decreases significantly for aged mice (0.58 ± 0.03, $W = -1018$, $p = 0.0004$; Fig. 5D) but does not do so for young adult mice (0.79 ± 0.06, $W = -90$, $p = 0.284$; Fig. 5D). This decrease in remodeling within clusters for aged mice is likely due to a decrease in spines being gained into clusters (prestimulation: 0.90 ± 0.03, post-stimulation: 0.73 ± 0.05, $W = -333$, $p = 0.0012$; Fig. 5E) rather than spines being eliminated from clusters (prestimulation: 0.86 ± 0.04, post-stimulation: 0.81 ± 0.04, $W = -146$, $p = 0.3916$; Fig. 5F). Together, these data suggest that although whisker stimulation reduces spine rearrangement in aged mice, the structural remodeling that remains is occurring with increasing rate outside of clusters and may not benefit from the spine-stabilizing reported to occur with spine clustering.

4. Discussion

4.1. Divergent shifts in dendritic spine dynamics after whisker stimulation

Our data reveal that in the absence of any manipulation, spine turnover rates are higher in the S1 of aged mice than those of young adult mice, as shown previously (Mostany et al., 2013). The results are significant because they reinforce that (1) some level of fluctuation in synaptic connectivity, and thus spines, is omnipresent and stochastic/activity-independent (Attardo et al., 2015; Loewenstein et al., 2015; Minerbi et al., 2009; Yasumatsu et al., 2008) and (2) measurements of spine dynamics after intervention must be viewed in terms of the deviation from their—perhaps already altered—steady-state levels.

Several studies have shown in vivo structural plasticity resulting from whisker-dependent manipulations (Alexander et al., 2018; Kuhlman et al., 2014; Wilbrecht et al., 2010; Zuo et al., 2005). However, this has never before been examined in the aged brain. Fixed tissue studies have been the main source of knowledge on the changes occurring in the aging brain for decades. However, owing to methodological limitations of fixed tissue, the study results were often contradictory. For example, spine density decreases have been reported in various species: rat (Bloss et al., 2011; Wallace et al., 2007), rhesus monkey (Dumitriu et al., 2010), and human (Jacobs et al., 1997) as well as spine density increases in rats (Connor et al., 1980) or mice (Benice et al., 2006). The present study was informed by our previous in vivo work showing elevated steady-state spine (postsynaptic) dynamics in S1 (Mostany et al., 2013) and in vivo work by others showing elevated cortical axonal bouton (presynaptic) dynamics (Grillo et al., 2013), together suggesting a more widespread phenomenon of elevated cortical synaptic dynamics in aged animals. The present study was designed to determine how these altered dynamics affect the aged brain's ability to structurally incorporate new sensory experiences. Our data indicate that whisker stimulation elicits diametric effects on spine dynamics for young adult and aged mice compared to their prestimulation baselines when examined at 4-day intervals: in young adults, these measures rose after stimulation, whereas in aged mice, these same measures decreased.

4.2. Unsuccessful rewiring of cortical circuits in aged mice

The successful incorporation of memories associated with new experiences is thought to depend on (1) the rewiring of neural circuits to incorporate these memories and (2) the persistence of these newly created circuits over time, forming a so-called "structural trace of memory" within the circuits' connective components (i.e., dendritic spines; Majewska et al., 2006; Hofer et al., 2009; Xu et al., 2009; Yang et al., 2009). Plasticity protocols are historically linked with short-term elevations in spine dynamics enabling reorganization of synapses after plasticity induction. Chessboard whisker deprivation increases spine turnover in S1BF (Trachtenberg et al., 2002), whereas monocular deprivation (Hofer et al., 2009) and learning of a novel motor task (Xu et al., 2009) dramatically increase spine gain in the visual and motor cortices, respectively. Thus, the reduction in spine dynamics seen in aged mice after whisker stimulation suggests a failure to form a structural trace associated with the new experience and modify the existing neuronal connectivity.

Before this work, it was unclear whether the structural evidence of plasticity in aged mice should be an increase in spine dynamics, parallel to that observed in young adults, resulting in even higher rates of spine gain, elimination, and turnover. Although young adults experience a heightened level of synaptic instability during states of plasticity, the implication of higher spine turnover at steady state may be that aged animals experience this synaptic instability as the norm. There is, perhaps, a ceiling effect when it comes to states of structural plasticity. If the spines of an aged animal are already responding during the baseline state as if they are undergoing plasticity, the system could either (1) be overdriven and simply not respond to further stimuli or (2) display a homeostatic response to maintain balance (Calì et al., 2018; Kirov et al., 2004; Kirov and Harris, 1999; Mahoney et al., 2014; Turrigiano et al., 1998).

4.3. Lack of enduring structural traces in aging

Our examination of spine dynamics one month after the whisker stimulation reveals a maintained decrease in spine TOR for aged mice. Although the longer-term reduction in spine dynamics seen in aged mice suggests less—perhaps aberrant—rewiring of cortical circuits than exhibited in their baseline state, it could also indicate a general absence of cortical rewiring for aged mice upon exposure to new sensory experiences. A more meaningful indicator of sensory encoding may be the persistence of their spines over time. Our study of spine lifetimes, however, shows that spines of aged mice are less persistent, presenting shorter half-lives, than their young adult counterparts. When we restrict this examination to newly formed spines, we observe that aged spines are less persistent than those of young adult mice and additionally display decreased persistence after whisker stimulation. This suggests that if circuit rewiring does occur after whisker stimulation in aged mice, it is not sustained.

4.4. Spine clustering and synapse stabilization

Spine clustering has been linked with synapse stabilization after plasticity (Frank et al., 2018), possibly because of coactivation of spines within the immediate proximity, plasticity cross-talk (Takahashi et al., 2012), and lowered LTP thresholds (Harvey and Svoboda, 2007; Makino and Malinow, 2011). The spread of depolarization (e.g., Ca^{2+}/NMDA spikes; Larkum and Nevian, 2008; Druckmann et al., 2014; Lee et al., 2016) along the dendrite and biochemical activity (e.g., spread of Ras activity; Yasuda et al., 2006; Harvey et al., 2008) likely underlie these phenomena. Because these forms of activity are not detectable in the imaging data generated by the present study, we developed a strategy for identifying putative spine clusters based on their spatial arrangement. We believe that our method for identifying spine clusters is a reasonable approach because the basic metrics, such as cluster length and density, calculated with our method are consistent with those reported by other studies that describe clusters using both spatial (Chen et al., 2012; Frank et al., 2018; Fu et al., 2012) and functional strategies (Harvey and Svoboda, 2007; Makino and Malinow, 2011).

Interestingly, these steady-state metrics of spine clustering are unaffected by aging, indicating that the aged dendrite can maintain normal spatial arrangements while unchallenged by induced plasticity, even in the face of the aging-related increase in steady-state spine dynamics. However, the density of spine clusters on aged dendrites is reduced after whisker stimulation, suggesting that sensory stimulation disrupts previously presented clusters. After plasticity induction, spine turnover on the aged dendrite is reduced largely because of a decrease in spine formation. Not only are fewer spines formed, but a smaller proportion of those new spines are located within clusters. Combined with unchanged spine elimination, the aged dendrite experiences a decrease in spine density and spine cluster density, as is depicted here (Fig. 6).

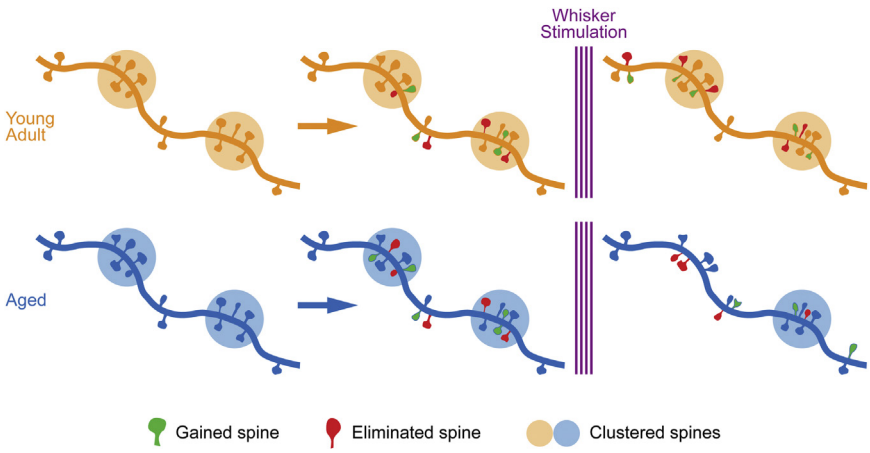

Fig. 6. Model showing decreased spine dynamics and clustering in aged mice after whisker stimulation. Schematic showing dendritic fragments from young adult mouse (top row, orange) and aged mouse (bottom row, blue). Schematic shows higher dendritic spine turnover (spines gained + eliminated) in aged mice before stimulation. After stimulation: young adult mice increase their dendritic spine turnover while cluster density remains stable. In aged mice: dendritic spine turnover and cluster density decreases after stimulation. Spines that are gained after stimulation occur more frequently outside of clusters.

Therefore, it is possible that lost spines belonging to a putative functional cluster are being replaced on the same dendrite by spines physically distant from the same cluster or other clusters. Perhaps, the elevated prestimulation spine dynamics in the aged dendrite were compensating for this relatively indiscriminate positioning of newly formed spines. The decrease in spine cluster density coupled with the increase in spine dynamics occurring outside of clusters suggests that aged mice are not employing clustering as a means of spine rearrangement after sensory stimulation. An increase in the fraction of new spines appearing in segments of the dendrite physically distant from functional clusters, where biochemical resources essential to stabilize synapses are less concentrated, may lead to the observed decrease in new spine survival. Although these phenomena have strong potential implications for spine behavior, it is important to note that these effects are dependent upon temporal coactivations of spines, a metric not captured here and a potential area of further study.

4.5. Reduced spine dynamics after whisker stimulation as a maladaptive compensation by aged mice

The 24-hour imaging data suggest that the effect of whisker stimulation on spines of aged animals is gradual and thus observed more clearly over a longer timeframe, when cumulative effects become increasingly visible. Daily imaging of young adult mice shows parallel increases in spine dynamics (+d1) roughly consistent with +d4 of the four-day interval timeline and a return to a baseline (+d2-4) roughly equivalent to +d8-12 of the four-day interval timeline. Aged mice, however, display a weaker response to whisker stimulation over the 24-hour timeline, with the parallel decrease in spine dynamics visible only after stimulation ceased.

Our original interpretation was that the reduction in spine dynamics in aged mice after whisker stimulation could be a compensatory measure to attenuate the synaptic instability present at baseline levels. Indeed, a larger phenomenon exists involving modest reversals or delays of neurodegeneration or cognitive deficits with sensory stimulation treatment. Improved performance on memory tasks is seen in humans with noninvasive transcranial stimulation (Flöel et al., 2012) and in rodents (Frick and Fernandez, 2003; Speisman et al., 2013) exposed to enriched environments. However, if this were the case, we should see concurrent indicators of improved spine stability in our experiments, including individual spine persistence and synaptic strengthening via clustering, both of which we fail to observe.

4.6. Synaptic tenacity versus plasticity

Spine dynamics are associated with a continuum between tenacity (circuit integrity) and plasticity (ability to remodel). Deficits in the aged brain may reflect an inability to maintain balance between these 2 circuit properties, in which compensations arise to maintain one side of this continuum while sacrificing the other. A reduction of spine dynamics in aged mice may not reflect a true stabilization of synapses but rather a failed attempt to maintain existing circuits and resist further changes, as has been observed in the prefrontal cortex (Bloss et al., 2010, 2011).

4.7. Somatosensory-specific deficits

We selected S1BF based on the experimental ability to monitor structural changes resulting from whisker-based manipulations and its suitability for characterizing potential age-related sensory deficits in future studies. These include examining the relationship between altered spine dynamics and sensory processing deficits through a behavioral paradigm to determine if the inability of aged mice to structurally incorporate a behavior correlates with declined performance. Although the effects regarding spine dynamics observed here may serve as a model for cortical circuits (or potentially for circuits across the brain) for how information may be stored within the structure of those circuits in later life, it is important to consider contributing factors that may either be somatosensory specific. Because the whisker stimulation is performed under anesthesia, a behavioral protocol under awake conditions could parse out potential upstream contributors from the larger sensory circuit including the posterior medial and ventral posterior medial divisions of the thalamus (Barthó et al., 2002; Constantinople and Bruno, 2011; Lavallée et al., 2005; Mease et al., 2016b; Trageser and Keller, 2004). Another area of interest might be the differences involving multiwhisker stimulation, which has implications for nonlinear integration of multiple information streams involving the barrel (above each whisker) and septal (in between the whiskers) regions of the somatosensory cortex (Ghazanfar and Nicolelis, 1997; Estebanez et al., 2016, 2018).

In summary, we provide the first evidence linking experience-dependent plasticity with in vivo spine dynamics in the aged brain. Aged mice display reduced spine dynamics, spine persistence, and spine clustering after stimulation, demonstrating reduced plasticity and failure to structurally incorporate new sensory experiences.

Disclosure

The authors have no actual or potential conflict of interest.

Acknowledgements

The authors would like to thank Drs. Pierre Apostolides, Randy Chitwood, Jennifer Siegel, and William Wimley, and members of the Mostany laboratory for guidance and helpful discussion.

This work was supported by a Louisiana Board of Regents Graduate Research Fellowship (LEQSF(2013-18)-GF-17) to RV and by grants from the National Institute on Aging (R01AG047296), Louisiana Board of Regents RCS (LEQSF(2016-19)-RD-A-24), and by the COBRE on Aging and Regenerative Medicine (P20GM103629) to RM.

References

Alexander, B.H., Barnes, H.M., Trimmer, E., Davidson, A.M., Ogola, B.O., Lindsey, S., Mostany, R., 2018. Stable density and dynamics of dendritic spines of cortical neurons across the estrous cycle while expressing differential levels of sensory-evoked plasticity. Front Mol. Neurosci. 11, 83.

Attardo, A., Fitzgerald, J.E., Schnitzer, M.J., 2015. Impermanence of dendritic spines in live adult CA1 hippocampus. Nature 523, 592–596.

Barthó, P., Freund, T.F., Acsády, L., 2002. Selective GABAergic innervation of thalamic nuclei from zona incerta. Eur. J. Neurosci. 16, 999–1014.

Benice, T.S., Rizk, A., Kohama, S., Pfankuch, T., Raber, J., 2006. Sex-differences in age-related cognitive decline in C57BL/6J mice associated with increased brain microtubule-associated protein 2 and synaptophysin immunoreactivity. Neuroscience 137, 413–423.

Bloss, E.B., Janssen, W.G., McEwen, B.S., Morrison, J.H., 2010. Interactive effects of stress and aging on structural plasticity in the prefrontal cortex. J. Neurosci. 30, 6726–6731.

Bloss, E.B., Janssen, W.G., Ohm, D.T., Yuk, F.J., Wadsworth, S., Saardi, K.M., McEwen, B.S., Morrison, J.H., 2011. Evidence for reduced experience-dependent dendritic spine plasticity in the aging prefrontal cortex. J. Neurosci. 31, 7831–7839.

Bloss, E.B., Puri, R., Yuk, F., Punsoni, M., Hara, Y., Janssen, W.G., McEwen, B.S., Morrison, J.H., 2013. Morphological and molecular changes in aging rat prelimbic prefrontal cortical synapses. Neurobiol. Aging 34, 200–210.

Burke, S.N., Barnes, C.A., 2006. Neural plasticity in the ageing brain. Nat. Rev. Neurosci. 7, 30–40.

Calì, C., Wawrzyniak, M., Becker, C., Maco, B., Cantoni, M., Jorstad, A., Nigro, B., Grillo, F., De Paola, V., Fua, P., Knott, G.W., 2018. The effects of aging on neuropil structure in mouse somatosensory cortex—a 3D electron microscopy analysis of layer 1 Ginsberg SD. PLoS One 13, e0198131.

Carvell, G.E., Simons, D.J., 1990. Biometric analyses of vibrissal tactile discrimination in the rat. J. Neurosci. 10, 2638–2648.
Cauller, L.J., Clancy, B., Connors, B.W., 1998. Backward cortical projections to primary somatosensory cortex in rats extend long horizontal axons in layer I. J. Comp. Neurol. 390, 297–310.
Chen, J.L., Villa, K.L., Cha, J.W., So, P.T.C., Kubota, Y., Nedivi, E., 2012. Clustered dynamics of inhibitory synapses and dendritic spines in the adult neocortex. Neuron 74, 361–373.
Connor, J.R., Diamond, M.C., Johnson, R.E., 1980. Aging and environmental influences on two types of dendritic spines in the rat occipital cortex. Exp. Neurol. 70, 371–379.
Constantinople, C.M., Bruno, R.M., 2011. Effects and mechanisms of wakefulness on local cortical networks. Neuron 69, 1061–1068.
Constantinople, C.M., Bruno, R.M., 2013. Deep cortical layers are activated directly by thalamus. Science 340, 1591–1594.
Druckmann, S., Feng, L., Lee, B., Yook, C., Zhao, T., Magee, J.C., Kim, J., 2014. Structured synaptic connectivity between hippocampal regions. Neuron 81, 629–640.
Dumitriu, D., Hao, J., Hara, Y., Kaufmann, J., Janssen, W.G.M., Lou, W., Rapp, P.R., Morrison, J.H., 2010. Selective changes in thin spine density and morphology in monkey prefrontal cortex correlate with aging-related cognitive impairment. J. Neurosci. 30, 7507–7515.
Estebanez, L., Bertherat, J., Shulz, D.E., Bourdieu, L., Léger, J.-F., 2016. A radial map of multi-whisker correlation selectivity in the rat barrel cortex. Nat. Commun. 7, 13528.
Estebanez, L., Férézou, I., Ego-Stengel, V., Shulz, D.E., 2018. Representation of tactile scenes in the rodent barrel cortex. Neuroscience 368, 81–94.
Feng, G., Mellor, R.H., Bernstein, M., Keller-Peck, C., Nguyen, Q.T., Wallace, M., Nerbonne, J.M., Lichtman, J.W., Sanes, J.R., 2000. Imaging neuronal subsets in transgenic mice expressing multiple spectral variants of GFP. Neuron 28, 41–51.
Flöel, A., Suttorp, W., Kohl, O., Kürten, J., Lohmann, H., Breitenstein, C., Knecht, S., 2012. Non-invasive brain stimulation improves object-location learning in the elderly. Neurobiol. Aging 33, 1682–1689.
Foster, T.C., 1999. Involvement of hippocampal synaptic plasticity in age-related memory decline. Brain Res. Brain Res. Rev. 30, 236–249.
Frank, A.C., Huang, S., Zhou, M., Gdalyahu, A., Kastellakis, G., Silva, T.K., Lu, E., Wen, X., Poirazi, P., Trachtenberg, J.T., Silva, A.J., 2018. Hotspots of dendritic spine turnover facilitate clustered spine addition and learning and memory. Nat. Commun. 9, 422.
Frick, K.M., Fernandez, S.M., 2003. Enrichment enhances spatial memory and increases synaptophysin levels in aged female mice. Neurobiol. Aging 24, 615–626.
Fu, M., Yu, X., Lu, J., Zuo, Y., 2012. Repetitive motor learning induces coordinated formation of clustered dendritic spines in vivo. Nature 483, 92–95.
Gambino, F., Pagès, S., Kehayas, V., Baptista, D., Tatti, R., Carleton, A., Holtmaat, A., 2014. Sensory-evoked LTP driven by dendritic plateau potentials in vivo. Nature 515, 116–119.
Ghazanfar, A.A., Nicolelis, M.A.L., 1997. Nonlinear processing of tactile information in the thalamocortical loop. J Neurophysiol. 78, 506–510.
Greenwood, P.M., 2007. Functional plasticity in cognitive aging: review and hypothesis. Neuropsychology 21, 657–673.
Grillo, F.W., Song, S., Teles-Grilo Ruivo, L.M., Huang, L., Gao, G., Knott, G.W., Maco, B., Ferretti, V., Thompson, D., Little, G.E., De Paola, V., 2013. Increased axonal bouton dynamics in the aging mouse cortex. Proc. Natl. Acad. Sci. U. S. A. 110, E1514–E1523.
Harris, K.M., Stevens, J.K., 1989. Dendritic spines of CA 1 pyramidal cells in the rat hippocampus: serial electron microscopy with reference to their biophysical characteristics. J. Neurosci. 9, 2982–2997.
Harvey, C.D., Svoboda, K., 2007. Locally dynamic synaptic learning rules in pyramidal neuron dendrites. Nature 450, 1195–1200.
Harvey, C.D., Yasuda, R., Zhong, H., Svoboda, K., 2008. The spread of Ras activity triggered by activation of a single dendritic spine. Science 321, 136–140.
Hofer, S.B., Mrsic-Flogel, T.D., Bonhoeffer, T., Hübener, M., 2009. Experience leaves a lasting structural trace in cortical circuits. Nature 457, 313–317.
Holtmaat, A., Bonhoeffer, T., Chow, D.K., Chuckowree, J., De Paola, V., Hofer, S.B., Hübener, M., Keck, T., Knott, G., Lee, W.-C.A., Mostany, R., Mrsic-Flogel, T.D., Nedivi, E., Portera-Cailliau, C., Svoboda, K., Trachtenberg, J.T., Wilbrecht, L., 2009. Long-term, high-resolution imaging in the mouse neocortex through a chronic cranial window. Nat. Protoc. 4, 1128–1144.
Holtmaat, A., Wilbrecht, L., Knott, G.W., Welker, E., Svoboda, K., 2006. Experience-dependent and cell-type-specific spine growth in the neocortex. Nature 441, 979–983.
Hooks, B.M., Hires, S.A., Zhang, Y.-X., Huber, D., Petreanu, L., Svoboda, K., Shepherd, G.M.G., 2011. Laminar analysis of excitatory local circuits in vibrissal motor and sensory cortical areas Petersen CCCH. PLoS Biol. 9, e1000572.
Jacobs, B., Driscoll, L., Schall, M., 1997. Life-span dendritic and spine changes in areas 10 and 18 of human cortex: a quantitative Golgi study. J. Comp. Neurol. 386, 661–680.
Johnston, D.G., Denizet, M., Mostany, R., Portera-Cailliau, C., 2013. Chronic in vivo imaging shows no evidence of dendritic plasticity or functional remapping in the contralesional cortex after stroke. Cereb. Cortex 23, 751–762.
Kirov, S.A., Goddard, C.A., Harris, K.M., 2004. Age-dependence in the homeostatic upregulation of hippocampal dendritic spine number during blocked synaptic transmission. Neuropharmacology 47, 640–648.
Kirov, S.A., Harris, K.M., 1999. Dendrites are more spiny on mature hippocampal neurons when synapses are inactivated. Nat. Neurosci. 2, 878–883.
Kuhlman, S.J., O'Connor, D.H., Fox, K., Svoboda, K., 2014. Structural plasticity within the barrel cortex during initial phases of whisker-dependent learning. J. Neurosci. 34, 6078–6083.
Larkum, M.E., Nevian, T., 2008. Synaptic clustering by dendritic signalling mechanisms. Curr. Opin. Neurobiol. 18, 321–331.
Lavallée, P., Urbain, N., Dufresne, C., Bokor, H., Acsády, L., Deschênes, M., 2005. Feedforward inhibitory control of sensory information in higher-order thalamic nuclei. J. Neurosci. 25, 7489–7498.
Lee, K.F., Soares, C., Thivierge, J.-P., Béïque, J.-C., 2016. Correlated Synaptic Inputs Drive Dendritic Calcium Amplification Coop. Plasticity during Clustered Synapse Development. Neuron 89, 784–799.
Lee, S., Kruglikov, I., Huang, Z.J., Fishell, G., Rudy, B., 2013. A disinhibitory circuit mediates motor integration in the somatosensory cortex. Nat. Neurosci. 16, 1662–1670.
Loewenstein, Y., Yanover, U., Rumpel, S., 2015. Predicting the dynamics of network connectivity in the neocortex. J. Neurosci. 35, 12535–12544.
Mahoney, R.E., Rawson, J.M., Eaton, B.A., 2014. An age-dependent change in the set point of synaptic homeostasis. J. Neurosci. 34, 2111–2119.
Majewska, A.K., Newton, J.R., Sur, M., 2006. Remodeling of synaptic structure in sensory cortical areas in vivo. J. Neurosci. 26, 3021–3029.
Makino, H., Malinow, R., 2011. Compartmentalized versus global synaptic plasticity on dendrites controlled by experience. Neuron 72, 1001–1011.
Mease, R.A., Metz, M., Groh, A., 2016a. Cortical sensory responses are enhanced by the higher-order thalamus. Cell Rep. 14, 208–215.
Mease, R.A., Sumser, A., Sakmann, B., Groh, A., 2016b. Cortical dependence of whisker responses in posterior medial thalamus in vivo. Cereb. Cortex 26, 3534–3543.
Megevand, P., Troncoso, E., Quairiaux, C., Muller, D., Michel, C.M., Kiss, J.Z., 2009. Long-term plasticity in mouse sensorimotor circuits after rhythmic whisker stimulation. J. Neurosci. 29, 5326–5335.
Minerbi, A., Kahana, R., Goldfeld, L., Kaufman, M., Marom, S., Ziv, N.E., 2009. Long-term relationships between synaptic tenacity, synaptic remodeling, and network activity. In: Stevens, C.F. (Ed.), PLoS Biol. 7, e1000136.
Mostany, R., Anstey, J.E., Crump, K.L., Maco, B., Knott, G., Portera-Cailliau, C., 2013. Altered synaptic dynamics during normal brain aging. J. Neurosci. 33, 4094–4104.
Mostany, R., Chowdhury, T.G., Johnston, D.G., Portonovo, S.A., Carmichael, S.T., Portera-Cailliau, C., 2010. Local hemodynamics dictate long-term dendritic plasticity in peri-infarct cortex. J. Neurosci. 30, 14116–14126.
Mostany, R., Portera-Cailliau, C., 2008. A method for 2-photon imaging of blood flow in the neocortex through a cranial window. J. Vis. Exp.
Patel, R.C., Larson, J., 2009. Impaired olfactory discrimination learning and decreased olfactory sensitivity in aged C57Bl/6 mice. Neurobiol. Aging 30, 829–837.
Pereira, A.C., Lambert, H.K., Grossman, Y.S., Dumitriu, D., Waldman, R., Jannetty, S.K., Calakos, K., Janssen, W.G., McEwen, B.S., Morrison, J.H., 2014. Glutamatergic regulation prevents hippocampal-dependent age-related cognitive decline through dendritic spine clustering. Proc. Natl. Acad. Sci. U. S. A. 111, 18733–18738.
Petreanu, L., Gutnisky, D.A., Huber, D., Xu, N., O'Connor, D.H., Tian, L., Looger, L., Svoboda, K., 2012. Activity in motor–sensory projections reveals distributed coding in somatosensation. Nature 489, 299–303.
Petreanu, L., Mao, T., Sternson, S.M., Svoboda, K., 2009. The subcellular organization of neocortical excitatory connections. Nature 457, 1142–1145.
Pologruto, T.A., Sabatini, B.L., Svoboda, K., 2003. ScanImage: flexible software for operating laser scanning microscopes. Biomed. Eng. Online 2, 13.
Speisman, R.B., Kumar, A., Rani, A., Pastoriza, J.M., Severance, J.E., Foster, T.C., Ormerod, B.K., 2013. Environmental enrichment restores neurogenesis and rapid acquisition in aged rats. Neurobiol. Aging 34, 263–274.
Spires-Jones, T.L., Meyer-Luehmann, M., Osetek, J.D., Jones, P.B., Stern, E.A., Bacskai, B.J., Hyman, B.T., 2007. Impaired spine stability underlies plaque-related spine loss in an Alzheimer's disease mouse model. Am. J. Pathol. 171, 1304–1311.
Spooner, R.K., Wiesman, A.I., Proskovec, A.L., Heinrichs-Graham, E., Wilson, T.W., 2018. Rhythmic spontaneous activity mediates the age-related decline in somatosensory function. Cereb. Cortex 29, 680–688.
Sweet, R.A., Henteleff, R.A., Zhang, W., Sampson, A.R., Lewis, D.A., 2009. Reduced dendritic spine density in auditory cortex of subjects with schizophrenia. Neuropsychopharmacology 34, 374–389.
Takahashi, N., Kitamura, K., Matsuo, N., Mayford, M., Kano, M., Matsuki, N., Ikegaya, Y., 2012. Locally synchronized synaptic inputs. Science 335, 353–356.
Thornbury, J.M., Mistretta, C.M., 1981. Tactile sensitivity as a function of age. J. Gerontol. 36, 34–39.
Trachtenberg, J.T., Chen, B.E., Knott, G.W., Feng, G., Sanes, J.R., Welker, E., Svoboda, K., 2002. Long-term in vivo imaging of experience-dependent synaptic plasticity in adult cortex. Nature 420, 788–794.
Trageser, J.C., Keller, A., 2004. Reducing the uncertainty: gating of peripheral inputs by zona incerta. J. Neurosci. 24, 8911–8915.
Turrigiano, G.G., Leslie, K.R., Desai, N.S., Rutherford, L.C., Nelson, S.B., 1998. Activity-dependent scaling of quantal amplitude in neocortical neurons. Nature 391, 892–896.
Veinante, P., Deschênes, M., 2003. Single-cell study of motor cortex projections to the barrel field in rats. J. Comp. Neurol. 464, 98–103.

Wallace, M., Frankfurt, M., Arellanos, A., Inagaki, T., Luine, V., 2007. Impaired recognition memory and decreased prefrontal cortex spine density in aged female rats. Ann. N. Y. Acad. Sci. 1097, 54–57.
Wilbrecht, L., Holtmaat, A., Wright, N., Fox, K., Svoboda, K., 2010. Structural plasticity underlies experience-dependent functional plasticity of cortical circuits. J. Neurosci. 30, 4927–4932.
Williams, L.E., Holtmaat, A., 2019. Higher-order thalamocortical inputs gate synaptic long-term potentiation via disinhibition. Neuron 101, 91–102.e4.
Xu, T., Yu, X., Perlik, A.J., Tobin, W.F., Zweig, J.A., Tennant, K., Jones, T., Zuo, Y., 2009. Rapid formation and selective stabilization of synapses for enduring motor memories. Nature 462, 915–919.
Yadav, A., Gao, Y.Z., Rodriguez, A., Dickstein, D.L., Wearne, S.L., Luebke, J.I., Hof, P.R., Weaver, C.M., 2012. Morphologic evidence for spatially clustered spines in apical dendrites of monkey neocortical pyramidal cells. J. Comp. Neurol. 520, 2888–2902.
Yang, G., Pan, F., Gan, W.-B., 2009. Stably maintained dendritic spines are associated with lifelong memories. Nature 462, 920–924.
Yasuda, R., Harvey, C.D., Zhong, H., Sobczyk, A., van Aelst, L., Svoboda, K., 2006. Supersensitive Ras activation in dendrites and spines revealed by two-photon fluorescence lifetime imaging. Nat. Neurosci. 9, 283–291.
Yasumatsu, N., Matsuzaki, M., Miyazaki, T., Noguchi, J., Kasai, H., 2008. Principles of long-term dynamics of dendritic spines. J. Neurosci. 28, 13592–13608.
Zhang, W., Bruno, R.M., 2019. High-order thalamic inputs to primary somatosensory cortex are stronger and longer lasting than cortical inputs. Elife 8.
Zuo, Y., Yang, G., Kwon, E., Gan, W.-B., 2005. Long-term sensory deprivation prevents dendritic spine loss in primary somatosensory cortex. Nature 436, 261–265.